

## Supplementary Information for “Molecular Origin of UV-Induced Irreversible Phase Changes in a Chromonic Liquid Crystal”

Junghoon Lee,<sup>1</sup> Seonghun Jeong,<sup>2</sup> Jung-min Kee,<sup>2,\*</sup> and Joonwoo Jeong<sup>1,3,†</sup>

<sup>1</sup>Department of Physics, Ulsan National Institute of Science and Technology, Ulsan, Republic of Korea

<sup>2</sup>Department of Chemistry, Ulsan National Institute of Science and Technology, Ulsan, Republic of Korea

<sup>3</sup>UNIST Research Center For Soft and Living Matter,

Ulsan National Institute of Science and Technology, Ulsan, Republic of Korea

(Dated: May 7, 2026)

### I. ABSORPTION SPECTRA OF SAMPLES

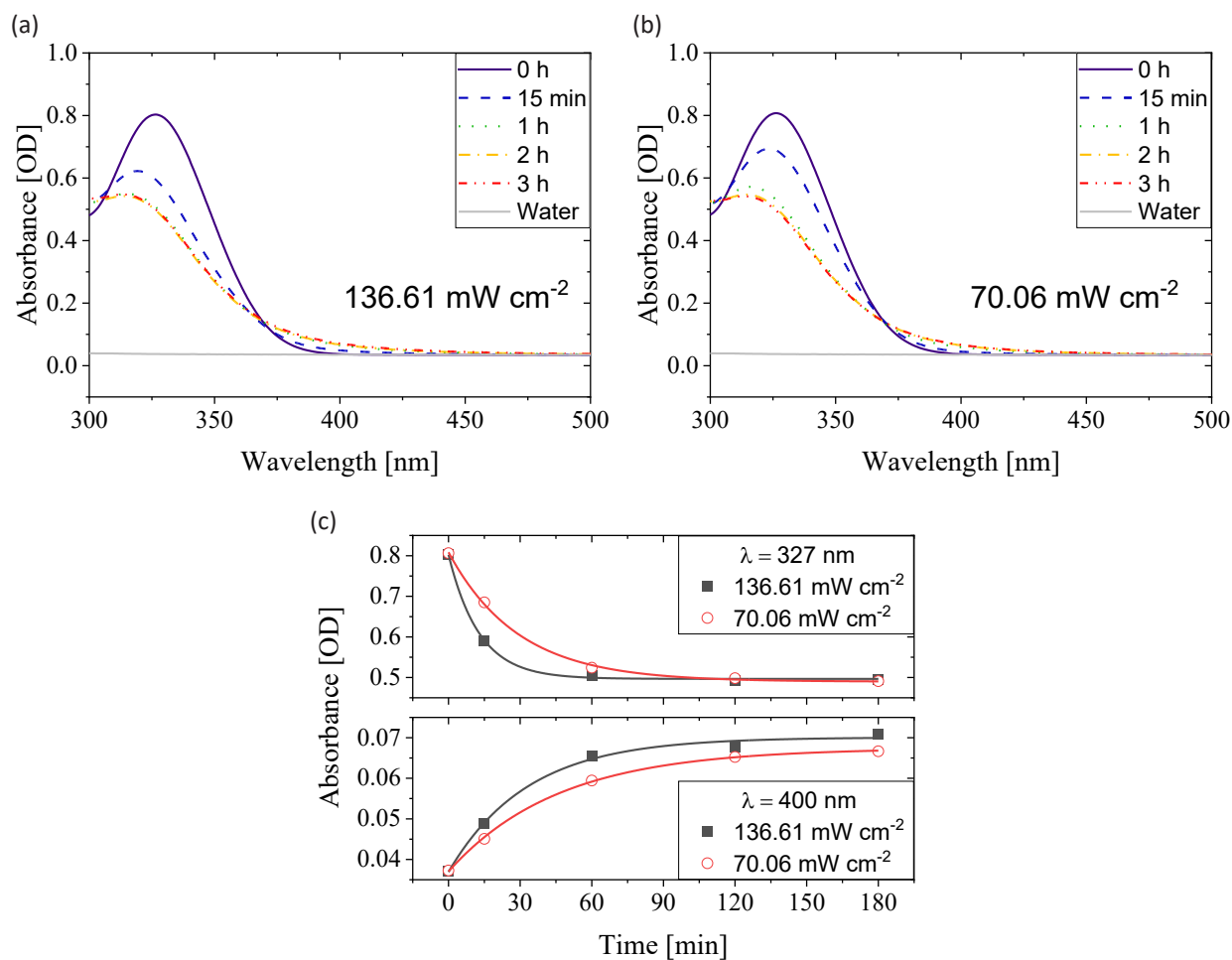


FIG. S1. Changes in UV-Vis absorption spectra of 0.1 wt% DSCG solutions under UV irradiation for 0–3 h at intensities of (a)  $136.61 \text{ mW cm}^{-2}$  and (b)  $70.06 \text{ mW cm}^{-2}$ . The gray line, for reference, shows the absorbance of deionized water in the same cuvette. (c) Exponential fits of the absorbance decreases at 327 nm and increases at 400 nm according to UV intensities.

The absorbance spectra of 0.1 wt% DSCG solutions in 0.5 mm path-length quartz cuvettes were acquired using a UV-Vis spectrometer (V-670, JASCO), according to the UV irradiation time in the range of 0–3 h. Note that we

\* jmkee@unist.ac.kr

† jjeong@unist.ac.kr

adjusted the sample concentration and optical path length to obtain reliable absorbance signals in the 300–500 nm range.

First, we analyze how the characteristic absorption peak at 327 nm, as assigned in Ref. [26], decreases with increasing UV illumination time and estimate the reaction rate constant  $k$  by fitting the signals to  $y(t) = y_0 + A_0 \exp(-kt)$ , where the absorbance  $y$  decays exponentially with two constants  $y_0$  and  $A_0$ . Here, we assume that the photodecomposition of DSCG follows apparent first-order kinetics,  $-\frac{d[\text{DSCG}]}{dt} = k[\text{DSCG}]$  and that the absorbance at 327 nm is proportional to the DSCG concentration [DSCG]. The rate constant decreased from  $k = (7.8 \pm 0.3) \times 10^{-2} \text{ min}^{-1}$  at a UV intensity of  $136.61 \text{ mW cm}^{-2}$  to  $k = (3.4 \pm 0.2) \times 10^{-2} \text{ min}^{-1}$  at  $70.06 \text{ mW cm}^{-2}$ , exhibiting approximate proportionality to the UV intensity.

As an empirical measure of the sample yellowing shown in Fig. 1(a), we analyze, in the same method, how the absorbance at 400 nm increases as a function of UV illumination time. At 400 nm, the corresponding rate constants for  $136.61 \text{ mW cm}^{-2}$  and  $70.06 \text{ mW cm}^{-2}$  are  $k = (3.0 \pm 0.5) \times 10^{-2} \text{ min}^{-1}$  and  $(2.2 \pm 0.1) \times 10^{-2} \text{ min}^{-1}$ , respectively; it shows a different proportionality from the one at 327 nm.

## II. AREA UNDER THE CURVE OF HPLC AND MASS SPECTRA OF LC-MS

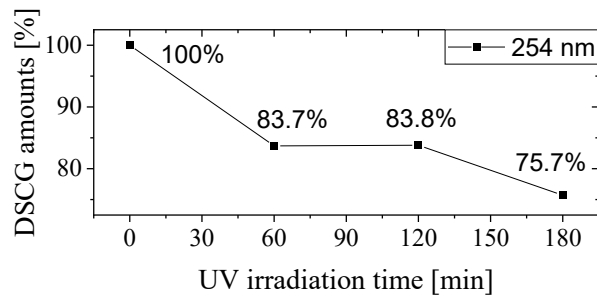


FIG. S2. Area under the curve (AUC) of the DSCG peak in the HPLC as a function of UV irradiation time. AUC, reflecting the amounts of DSCG, decreases as the UV irradiation time increases.

## III. LC-MS ANALYSIS

Here we provide the detailed data of our LC-MS analysis.

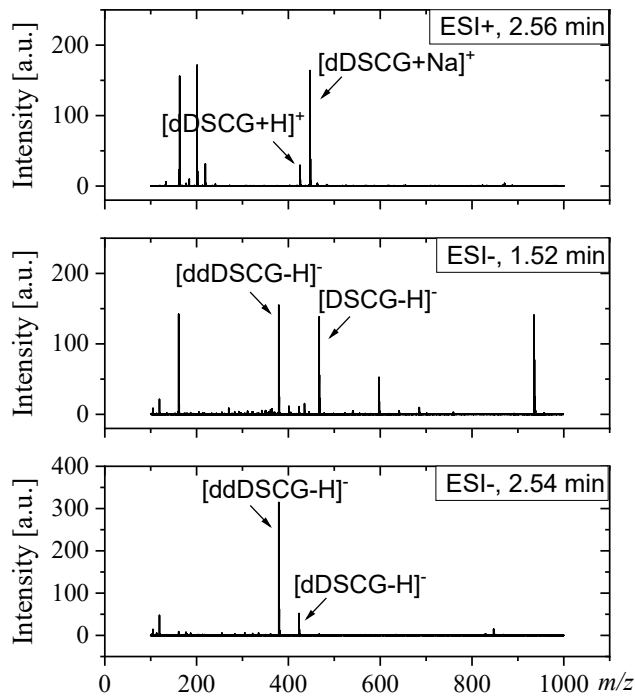


FIG. S3. LC-MS data of the DSCG sample after 10 hours of UV irradiation. We identify two photodegraded compounds: ddDSCG and dDSCG. Subsequent ESI-MS analysis in positive and negative ion modes, performed at the retention times of the newly emerged chromatographic peaks, identified  $m/z$  signals corresponding to the proposed photodegradation products shown in Fig. S4.

## IV. PROPOSED PHOTODEGRADATION PRODUCTS

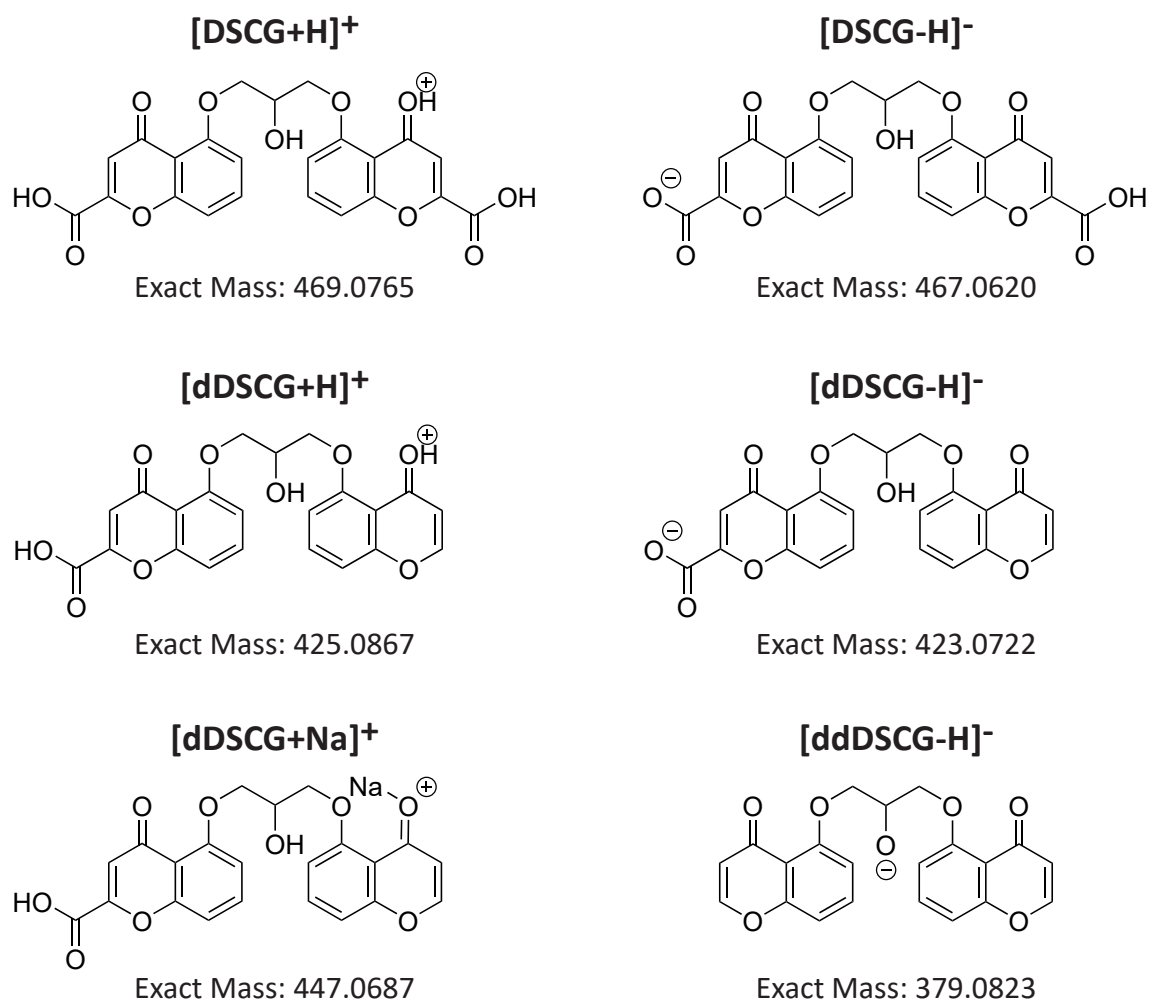


FIG. S4. Molecular masses and structures of DSCG-derived ions and proposed ionized photodegradation products.

## V. X-RAY SCATTERING DATA

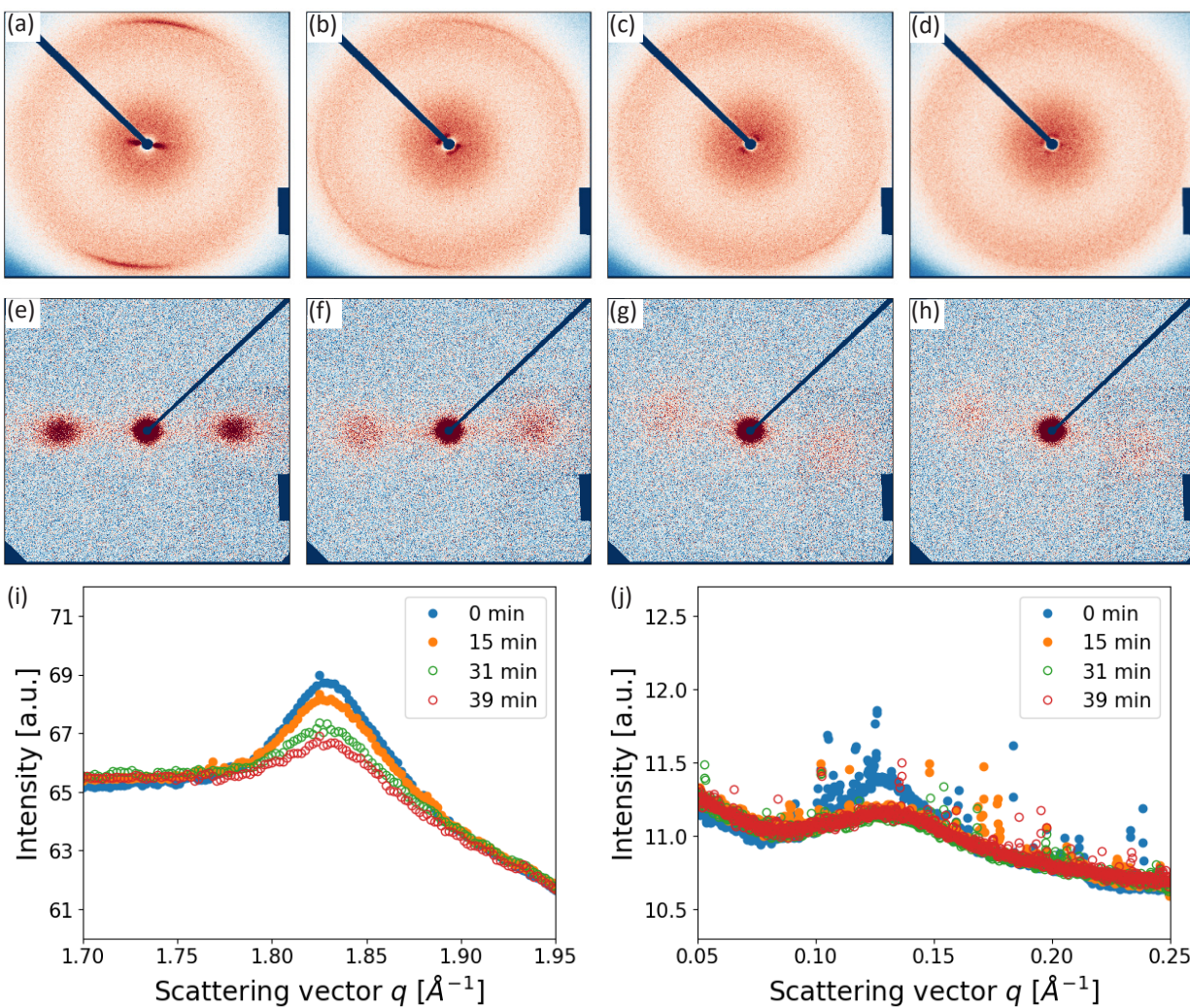


FIG. S5. Comparison of X-ray scattering data for samples subjected to UV irradiation. The entire sample area was uniformly illuminated. Panels (a,e) correspond to 0 min, (b,f) to 15 min, (c,g) to 30 min, and (d,h) to 39 min of irradiation. (a–d) In the wide-angle region, the scattering peak broadens while the intensity decreases compared to the neat sample shown in (a). (e–h) A similar trend is observed in the small-angle region. (i,j) show the azimuthally averaged intensity profiles.

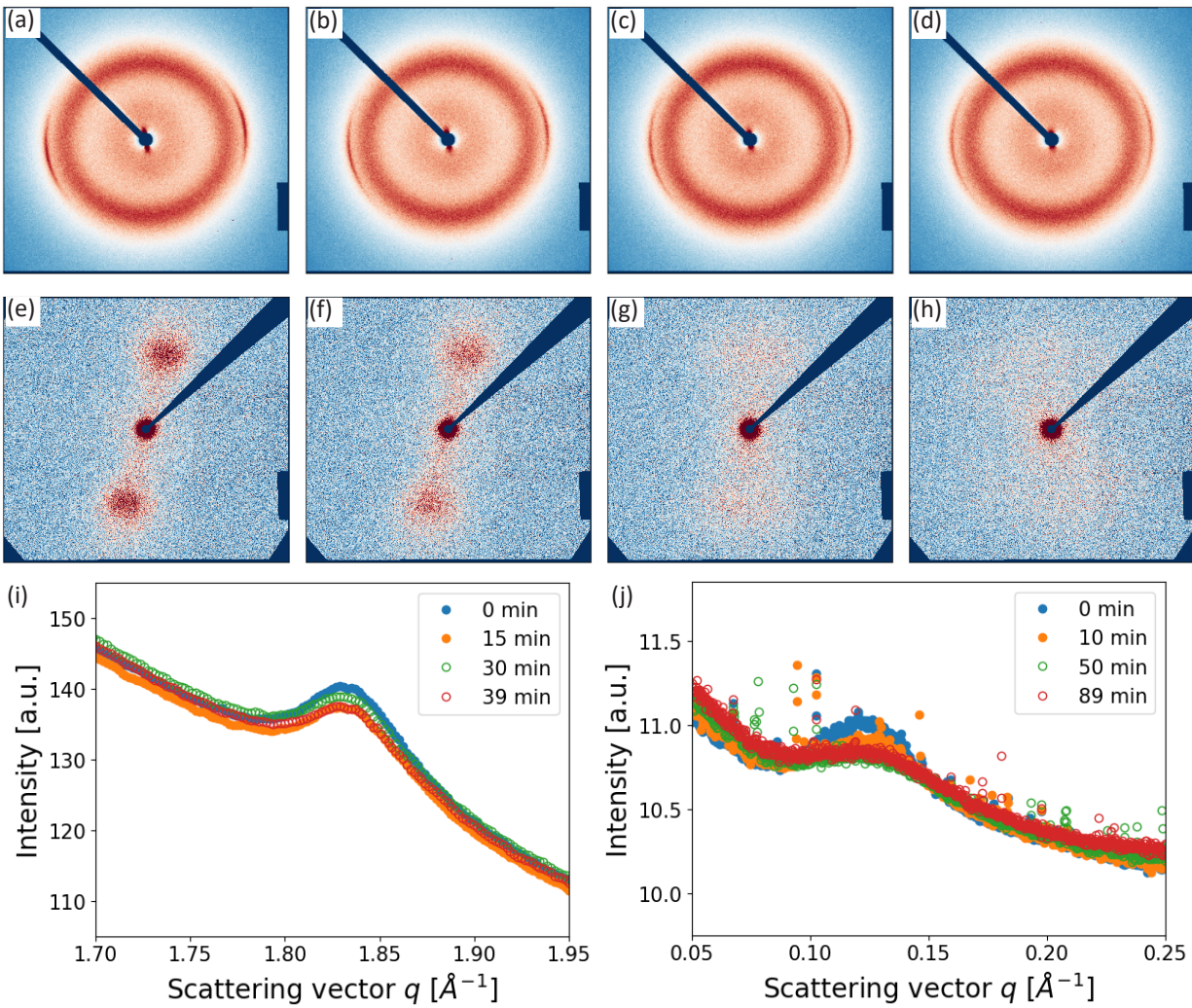


FIG. S6. Comparison of X-ray scattering data for samples subjected to local UV irradiation. The sample was illuminated only over a localized region. (a–d) In the wide-angle region, the scattering peak broadens while the intensity decreases relative to the initial sample. (e–h) A similar transformation is observed in the small-angle region. Note that the irradiation times used in the WAXD and SAXS measurements are different to achieve comparable UV-induced changes. Accordingly, panels (a–d) correspond to 0, 15, 30, and 39 min, whereas panels (e–h) correspond to 0, 15, 50, and 89 min. (i,j) show the azimuthally averaged intensity profiles.